energies

MDPI

Article

Study on Micro Topography of Thermal Aging of Insulation Pressboard Based on Image Processing

Liang Zhao [1], Wenhui Jiang [1], Yulong Wang [1], Ziqi Wang [2,*] and Yongqiang Wang [3]

[1] China Southern Grid Digital Grid Research Institute Co., Ltd., Guangzhou 510000, China
[2] School of Electrical and Electronic Engineering, North China Electric Power University, Baoding 071000, China
[3] Department of Electrical Engineering, North China Electric Power University, Baoding 071000, China
* Correspondence: wzq943275395@163.com

Abstract: The insulation pressboard is very important in the insulation of oil-immersed transformers, which determines the useful life of the transformer. In order to analyze the change in the micro topography of the pressboard under the condition of thermal aging in detail, the insulation pressboard samples of different thermal aging periods were made. Image enhancement, denoising, segmentation, optimization, edge detection, expansion, and corrosion were used to process SEM images of the pressboard after thermal aging, so as to extract the fiber width, hole size, and surface roughness. By comparing the relationship between the micro topography and the degree of polymerization of the insulation pressboard in different thermal aging periods, it can be concluded that when the fiber width was 91% of the unaged pressboard fiber width, and the corresponding roughness was 0.162, the insulation life was only approximately half of its original value, and when the fiber width was 79% of that of the unaged pressboard, the corresponding roughness was 0.225, and the insulation life was nearing the end of its life. This shows that the image processing method used in this paper can observe the micro topography changes during thermal aging and can estimate the thermal aging degree of the insulation pressboard.

Keywords: image processing; insulation pressboard; thermal aging; SEM image

Citation: Zhao, L.; Jiang, W.; Wang, Y.; Wang, Z.; Wang, Y. Study on Micro Topography of Thermal Aging of Insulation Pressboard Based on Image Processing. *Energies* **2022**, *15*, 6317. https://doi.org/10.3390/en15176317

Academic Editor: Mario Marchesoni

Received: 29 July 2022
Accepted: 25 August 2022
Published: 30 August 2022

1. Introduction

The inner insulation of an oil-immersed transformer is mainly made of oil-paper insulation, and the main insulation materials are insulating oil, insulating paper and cardboard. Cardboard insulation, as an important part of transformer insulation, determines the overall insulation of the transformer, and its role is prominent and significant. However, paperboard insulation is vulnerable to impact damage and difficult to recover, so paperboard insulation protection is particularly important [1,2].

With the development of cellulose microscopic theory and the continuous improvement of the precision of observation equipment, domestic and foreign workers began to study the aging and breakdown process of insulating boards from the microscopic perspective, which is of great significance to analyze its aging mechanism and improve the performance of insulating materials [3–5]. Using a scanning electron microscope (SEM) to observe the surface morphology of paperboard can intuitively analyze the advantages and disadvantages of the paperboard and fiber destruction process and the corresponding improvement. Liao Ruijin et al., through scanning electron microscope image analysis [6], found that the fiber width of insulating paper decreases after thermal aging, and with the development of partial discharge, the surface of the insulating paper displays "ablation", "peeling", "splitting", "pits", and "arborization". Yan Jiaming et al. proposed that the surface of the oil-immersed insulating paper develops damage over time, and "surface night drop" and "crystalline solid" form successively [7]. All of the above are direct observation results obtained from SEM images, but no further analysis of the deep statistical information has been conducted.

There are two ways to analyze SEM images: One is based on mature image processing software such as Photoshop, Mapinfo, IPP, GIS, and so on. The other is to write commands to process images based on Matlab, Visual C++, FORTRAN, and other mathematical function software [8]. At present, SEM images analyzed by image processing are mainly used for alloy, rock, and soil particles and pores [9–12]. Some scholars have conducted detailed studies on the detection method of insulator hydrophobicity images [13,14], but no relevant paper has analyzed the microstructure of insulating board SEM images in detail.

Based on the Matlab image processing functions, a detailed analysis was carried out on the insulation board SEM images, statistics of the cardboard microscopic information in all stages of thermal aging, and further study on the board surface microstructure such as the fiber width, hole size, and the trend of surface roughness change with aging. The corresponding conclusions and improved results are presented.

2. Test Method and Measurement

2.1. Preparation of Sample

In this paper, an 80 × 80 × 2 mm^3 standard insulating board produced by Weidmann Company of Switzerland (Rapperswil-Jona, Switzerland) was used as the aging sample (the influence of the board size on the uncertainty of test measurement was ignored), and karamay #25 transformer oil was used as test oil. The new insulating board was vacuum-dried and impregnated before use. The specific method was as follows: The insulating board sample was placed in the vacuum-drying oven, and the ion pump was used to vacuum the vacuum-drying oven. The internal temperature of the drying oven was set to 90 °C, the air pressure was 50 Pa, and the vacuum drying continued for 48 h. After that, karamay #25 transformer oil was injected, and the internal temperature of the drying oven was maintained at 80 °C, the air pressure was maintained at 50 Pa, and the vacuum impregnation continued for 24 h.

The pre-treated oil and paperboard were mixed at a mass ratio of 10:1 to accelerate aging at 130 °C. According to Montsinger's rule [15], insulation boards of different aging degrees are made for aging experiments, and the formula is as follows:

$$T = Ae^{-\alpha(\theta-\theta_0)} \quad (1)$$

where T is the insulation life at the actual working temperature; A is the insulation life at the reference operating temperature; θ is the actual working temperature of the insulation material, wherein 130 °C is taken here; and θ_0 is the reference working temperature of the insulating material. α is the thermal aging coefficient, generally 0.1155.

The paperboard underwent accelerated thermal aging for 0 days, 1 day, 2 days, 5 days, 8 days, 16 days, 20 days, 24 days, 32 days, and 48 days in the test, which is equivalent to 0 years, 0.88 years, 1.77 years, 4.41 years, 7.06 years, 14.12 years, 17.65 years, 21.18 years, 28.24 years, and 42.36 years, respectively, under the normal operation of the transformer. On the corresponding days, we took out appropriate amounts of the insulating board, vacuumed it three times to fully extract the aging oil sample in the board, and obtained insulating board samples of different degrees of aging. The degree of aging of cardboard can be characterized by the degree of cardboard polymerization.

2.2. Paperboard Polymerization Degree Measurement

It is generally believed that the degree of polymerization of new paperboard without aging is between 1000 and 1200. When the degree of polymerization of paperboard drops to approximately 500, the life of paperboard decreases to approximately half. When the degree of polymerization of cardboard drops to approximately 200~250, the life of cardboard has essentially reached the end of its service life [16]. According to GB/T 1548-2004, the paper measures the degree of polymerization of paperboard, and the basic steps are as follows:

(1) A sample of insulating board aged at different times was taken out, and the cable extractor was used for liposuction operation.

(2) We determined the outflow time of 50% Copper-ethylenediaminecomplex in an Ubbelohde viscometer.

(3) The insulating board after medium liposuction in (1) was dissolved in 50% Copper-ethylenediaminecomplex and fully stirred, and then the outflow time of different mixed solutions was measured in the Ubbelohde viscometer successively.

The viscosity ratio in the test can be obtained from the ratio of solution outflow time, as follows:

$$\eta_s = \frac{t_1 - t_0}{t_0} \tag{2}$$

where t_0 is the outflow time of a 50% cupric ethylenediamine aqueous solution, and t_1 is the outflow time of an insulating board dissolved in a 50% cupric ethylenediamine solution.

According to the viscosity ratio η_S, the value of $[\eta]\cdot C$ can be found according to the table provided by GB/T 1548-2004. The slurry concentration C can be calculated due to the sample mass and solution volume (50.0 mL), and the characteristic viscosity value $[\eta]$ can be obtained by dividing by C, as shown in Equation (3), as follows:

$$[\eta] = \frac{[\eta]\cdot C}{C} \tag{3}$$

where $[\eta]$ is the intrinsic viscosity; C is the pulp concentration (calculated from the mass of the insulating board and the volume of the solution).

According to the functional relationship between the polymerization degree DP and $[\eta]$, the polymerization degree of cardboard with different aging durations can be calculated:

$$DP^{0.905} = 0.75[\eta] \tag{4}$$

2.3. Measurement of Surface Topography

We removed the insulating cardboard samples aged at different times and placed them into a beaker filled with acetone for 10 min to dissolve the residual oil samples in the cardboard, and then put them into a vacuum-drying oven for drying. After drying, the insulating board does not conduct electricity, so a conductive film needs to be plated on the board's surface. The coating machine was an SBC-12 small ion sputtering instrument. After coating, a scanning electron microscope (MODEL EM-30PLUS) was used to analyze the surface morphology of the insulating paperboard at different stages of thermal aging.

The internal characteristics of the fiber, such as the fiber width, reflect the basic characteristics of the fiber form and affect the physical properties of the insulating board [17]. Generally, after a long duration of aging, cardboard's fiber width will be reduced to a certain extent. With the deepening of aging, the fiber cell wall of the insulating paperboard displays the phenomenon of splitting and longitudinal splitting, the fiber surface has holes, and its surface smoothness becomes worse. Therefore, the aging degree of the insulating board can be inferred by measuring the fiber width, hole size, and fiber surface roughness.

To avoid the insulation board forming cellulose, holes, and surface roughness due to the differences between different processing technologies, and to ensure the SEM image survey points to a representative, this paper selected, for each stage of thermal aging and with three copies of the insulation board, five sampling points in each insulating cardboard fiber width, hole size, and surface roughness measurement. The average fiber width and surface roughness of each aging stage were calculated, and the pore data of each aging stage were recorded, this is shown in Figure 1.

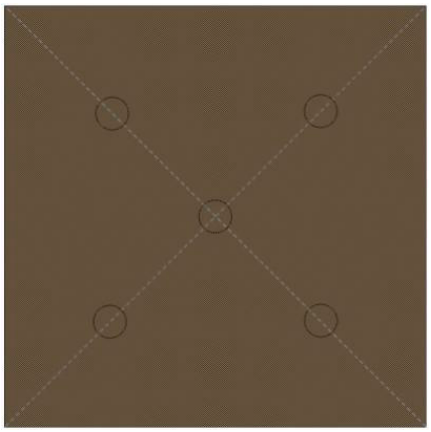

Figure 1. Sampling map of surface morphology of insulation pressboard.

3. Image Processing

Matlab internal contains a large number of functions, involving a number of toolboxes, including an image processing toolbox. The analysis of SEM images is mainly based on the functions in the image processing toolbox for research and measurement, and the specific algorithm flow is shown in Figure 2.

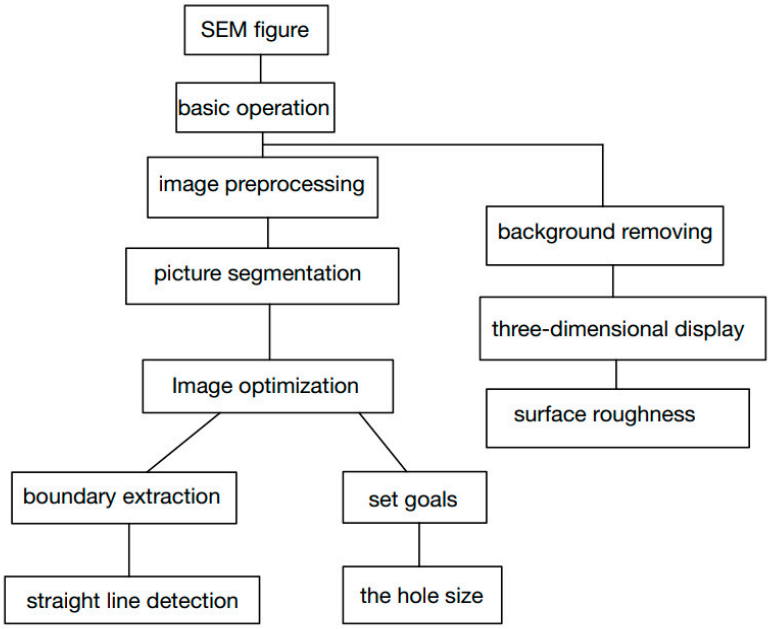

Figure 2. Flow diagram of image processing algorithm.

3.1. Wavelet Enhancement Algorithm

In the process of image scanning with the wavelet enhancement algorithm, the gray contrast of the image background and the target area is weak due to the poor contrast adjustment of the image and the close gray value of the fiber itself and part of the background. Therefore, the fiber and background rendering in the image are enhanced by enhancing the contrast of the image. Filtering enhancement can be implemented by the imnoise function, smoothing filter, median filter, two-dimensional statistical filter, and wavelet enhancement. Among them, the first four methods use a spatial template to move point by point in the image, and the response of the point is calculated by the relation between the filtering coefficient and the corresponding pixel value of the region swept by the filtering template. The basic idea of wavelet enhancement is to decompose an image into components with different sizes, positions, and directions. Before inverse transformation,

the low-frequency part reflecting the contour is enhanced, and the high-frequency part reflecting the details is attenuated, so as to achieve the purpose of image enhancement. SEM images are grayscale images with a great deal of noise, so it is difficult for traditional spatial filtering to achieve good results. However, wavelet enhancement can cover the whole frequency domain, and the correlation between different features can be effectively reduced by selecting appropriate filters and adjusting parameters.

3.1.1. Wavelet Decomposition

The wavelet function can be constructed from the parent wavelet $\Psi(x)$ defined on a finite interval.

$$\Psi_{ab}(x) = \left|\frac{1}{\sqrt{a}}\right| \Psi\left(\frac{x-b}{a}\right) \tag{5}$$

where a is the scale factor, reflecting the width of a specific basis function; b is the translation factor, specifying the position of the translation along the X-axis.

In the process of the wavelet transform, the wavelet basis function moves in parallel on the time axis, and the approximation degree of the original graphic signal and the wavelet function at every moment is calculated [18]. In wavelet decomposition, this paper adopts sym4, an improved approximate symmetric wavelet function based on DB function, as the parent wavelet [19], to carry out a two-layer discrete wavelet decomposition of images.

The first discrete wavelet decomposition process can be described as follows: Firstly, the discrete wavelet transform (DWT) is performed on each line of the image to obtain the low-frequency component L and high-frequency component H of the original image in the horizontal direction. Then, DWT is performed on each column of the transformed data to obtain the low-frequency components LL_1 in horizontal and vertical directions, LH_1 in horizontal and vertical directions, and HL_1 and HH_1 in horizontal and vertical directions. Then, the second layer of discrete wavelet decomposition is carried out, and the principle is the same as above.

An appropriate pixel threshold was set for the image after wavelet decomposition, and the part below the threshold was enhanced, while the part above the threshold was weakened.

3.1.2. Wavelet Reconstruction

Wavelet reconstruction is the inverse transform of the wavelet transform, which is the superposition of the approximate number and detail coefficient obtained by decomposition to obtain the original signal. The reconstruction process is as follows: First, the inverse one-dimensional discrete wavelet transform is carried out for each column of the transformation result, and then the inverse one-dimensional discrete wavelet transform is carried out for each row of the data obtained from the transformation to obtain the reconstructed image.

The first-layer wavelet decomposition and wavelet reconstruction process are shown in Figure 3.

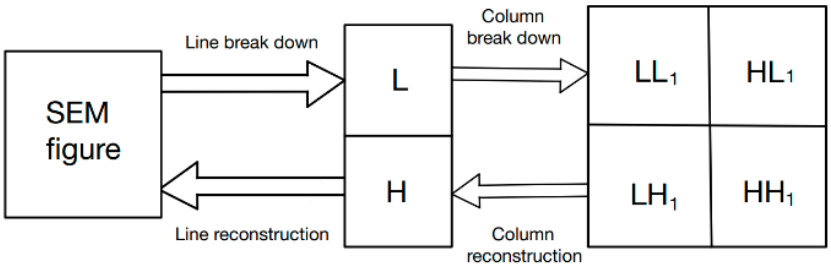

Figure 3. Flow diagram of wavelet decomposition and reconstruction.

3.2. Fingerprint Image Segmentation Method

Image segmentation, also known as image binarization, transforms a gray image into a black and white binarization image. The segmented image can only retain the contour

information of the fiber and hole but cannot describe the surface details of the fiber and hole. Therefore, experiments with various segmentation methods are needed to find the optimal method. In this paper, the algorithm is improved on the basis of an iterative threshold, and a local adaptive threshold segmentation algorithm based on reducing the block effect is proposed. The main steps are as follows:

(1) The image with a pixel of $M \times N$ is evenly divided into sub-images with a pixel of $m \times n$.

(2) Iterative threshold segmentation is performed for each sub-image [20]: Calculate the maximum gray value $Z_{\max}$ and minimum gray value $Z_{\min}$ of each sub-image, and the initial threshold T_0 is $(Z_{\max} + Z_{\min})/2$.

(3) T_i divides the image into the foreground and background, calculates the average gray value Z_1 and Z_2 of the two with Equation (6), and finds the new threshold $T_i = (Z_1 + Z_2)/2$.

$$\begin{cases} Z_1 = \dfrac{\sum\limits_{i=0}^{T_i} in_i}{\sum\limits_{i=0}^{T_i} n_i} \\ Z_2 = \dfrac{\sum\limits_{i=T_i}^{t-1} in_i}{\sum\limits_{i=T_i}^{t-1} n_i} \end{cases} \tag{6}$$

(4) Repeat step (3) until $T_K = T_{K+1}$, then the threshold is T_{K+1}.

(5) The equal spacing interpolation method is adopted to reduce the influence of the block effect: The threshold T_{ij} obtained in step (4) is stored at the starting position of the corresponding sub-image, the interval between two adjacent values in each column is inserted $\frac{T_{tf} - T_{t(f-1)}}{N/n}$, $(N/n - 1)$ values are expanded, the interval between two adjacent values in each row is inserted $\frac{T_{tf} - T_{(t-1)f}}{M/m}$, and the number of $(M/m - 1)$ values is expanded. Then, we insert $(N/n - 1)$ numbers with a value of T_{in} in each row of the last column of the obtained matrix, similarly insert $(M/m - 1)$ numbers with a value of T_{mj} in each column of the last row, and finally, obtain the image with the same number of pixels as the original image.

3.3. Test Measurement Content

3.3.1. Fiber Width

After image optimization, fiber edge detection is often carried out by spatially differential operators such as the gradient operator, Laplacian operator, and *Canny* operator. In this paper, the Laplace operator is selected to extract the fiber boundary after the actual comparison. The linear part of the fiber boundary can be detected by Hough transformation, as shown in Figure 4a. After that, the fiber width is quantitatively measured by the ruler in Matlab.

3.3.2. The Hole Size

Matlab has a large error in identifying holes in SEM images, so it is necessary to directly and interactively cut holes in cardboard fibers to ensure the accuracy of identifying holes. After image enhancement, segmentation, and optimization, the *bwboundaries* function was used to determine the boundaries of the holes. Then, the number of component pixels was calculated using the *regionprops* function to calculate the hole area. Figure 4b,c show the holes in the original picture after clipping and the holes with determined pixels, respectively.

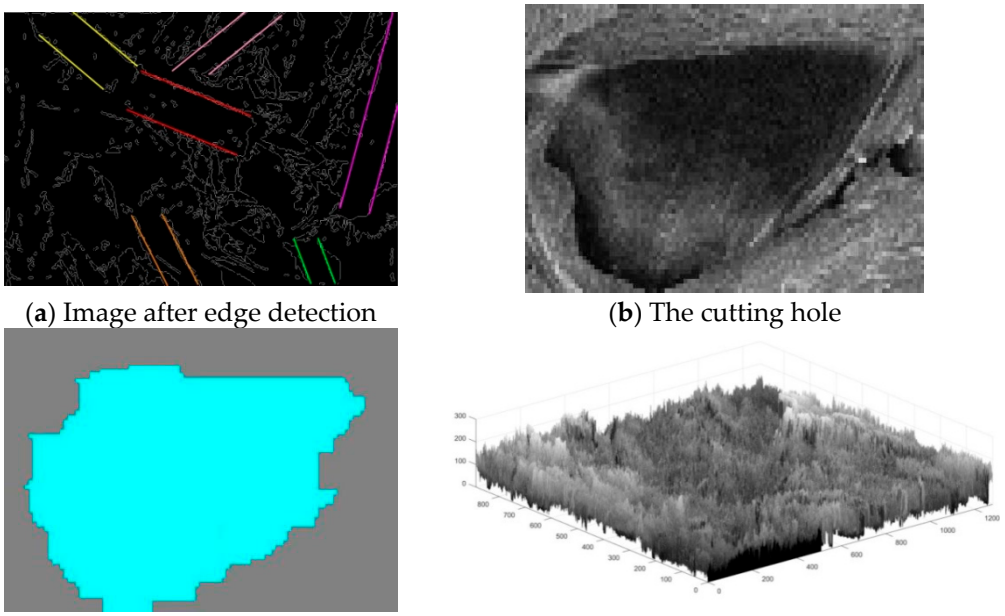

(**a**) Image after edge detection (**b**) The cutting hole

(**c**) Determine the hole behind the pixel (**d**) Three dimensional display of insulating board microstructure

Figure 4. The displays of measurement results.

3.3.3. Surface Roughness and 3D Display

The surface roughness of insulating cardboard is characterized by the three-dimensional arithmetic mean deviation Sa of the SEM image, and its calculation formula is [21]:

$$\begin{cases} Sa = \frac{1}{MN}\sum_{i=1}^{M}\sum_{j=1}^{N}\left|Z(x_i,y_j)-u\right| \\ u = \frac{1}{MN}\sum_{i=1}^{M}\sum_{j=1}^{N}Z(x_i,y_i) \end{cases} \quad (7)$$

where M and N are the discrete sampling points in the x and y directions, respectively, that is, the x and y values of the clipping image. u represents the mean of the discrete sampling points in x and y directions. For the convenience of observation and statistical comparison, the data have been normalized.

In the computer, the size of the SEM image is measured by the pixel size, and the height is expressed by the gray value. In the SEM image, the closer the particle is to the light source, the higher its pixel gray value is, which is brighter in the image. The farther away from the light source, the smaller the gray value, which is darker in the image. Therefore, each pixel can be used as the base, and their gray value can be increased to show the three-dimensional form of the image, as shown in Figure 4d.

4. Treatment Results and Analysis

On the basis of the image processing mentioned above, the surface microscopic morphology of the prepared SEM images of insulating cardboard in various aging stages was analyzed. The statistical results of the fiber width, hole size, and surface roughness are shown in Figure 5, Table 1, and Figure 6, respectively. Figure 5 shows the changing trend of the average fiber width over time. It can be seen that with the increase in aging days, the average fiber width gradually decreases from 40.5 μm before aging to 31.8 μm after 48 days of aging.

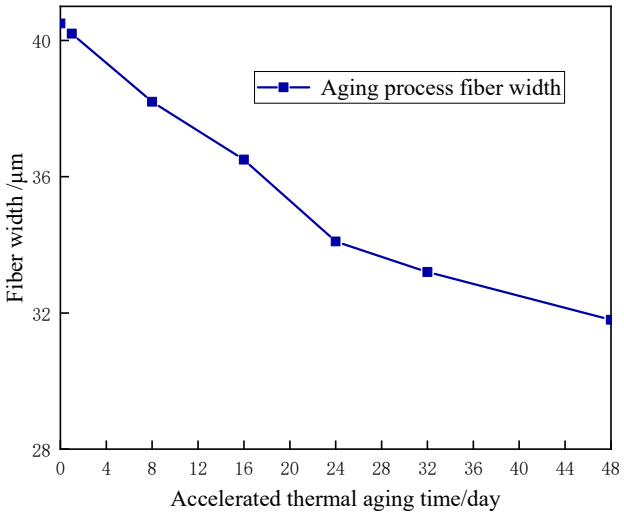

Figure 5. The average fiber width changes with time.

Table 1. Statistical results of hole area.

Accelerated Aging Time/Day	The Hole Size/μm^2			
	1	2	3	4
0 day	34.1			
8 days	48.7	129.5		
16 days	62.3	118.6	164.5	
32 days	89.3	204.6	463.1	
48 days	69.55	186.4	956.3	974.7

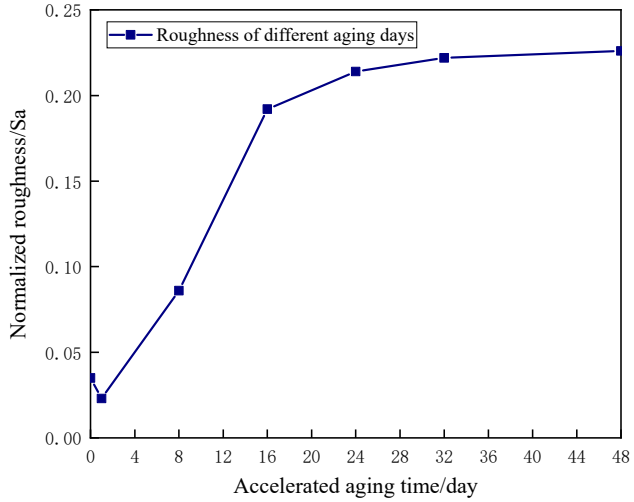

Figure 6. The surface roughness changes with time.

In Table 1, the hole area is measured by selecting an SEM image at each aging stage with a magnification of 1000 times under the scanning electron microscope and the image stored pixels at 1280 × 960 pixels, to illustrate the process of holes in different aging stages. It can be seen that with the increase in aging days, the number and area of holes also increase. The unaged insulating paper has only one hole, and the hole area is only 34.1 μm^2, while the sample aged for 48 days has four holes and the hole area is up to 974.7 μm^2.

Figure 6 shows the changing trend of surface roughness with aging time. It can be seen that from 0 to 2 days of aging, the normalized roughness decreases first, and from 2 days to 20 days of aging, the roughness gradually increases to 0.22, and then tends toward a stable value.

In order to evaluate the life of an insulating board, the change in polymerization degree of an insulating board during thermal aging was measured according to the viscosity method, and the relationship between the polymerization degree of the insulating board during aging and the fiber width and surface roughness is expressed in Figure 7. In Figure 7, the degree of polymerization of paperboard is 1050, as the reference standard. Surface roughness is normalized. The paper board fiber width takes the average fiber width of unaged paper board as the reference standard of 40.5 mm, and the above three items are expressed as percentages, so the variation trend chart of each parameter in the aging process can be obtained.

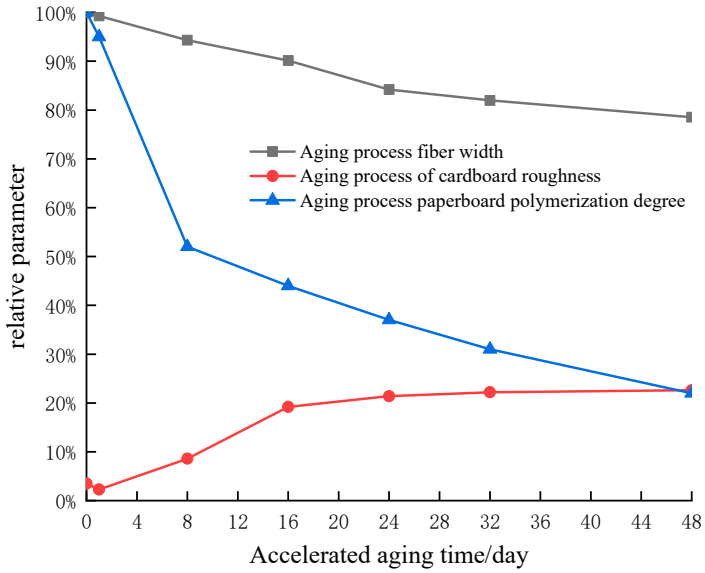

Figure 7. The trend of the various parameters during the aging process.

The degree of polymerization of the insulating board reflects its aging degree, so the degree of polymerization of the insulating board is taken as the statistic to evaluate the aging degree of the insulating board. As can be seen from Figure 7, when the degree of polymerization is close to 500, which is approximately 50% of the degree of polymerization of the original board, the aging time can be roughly inferred to be approximately 14 days, the insulation life is only approximately half, and the corresponding fiber width is approximately 37 μm (91% of the width of the fiber without aging), and the corresponding roughness is 0.162. When the degree of polymerization is close to 250, which is approximately 25% of the degree of polymerization of the original cardboard, it can be roughly inferred from Figure 7 that the aging time is approximately 45 days, which is close to the end of the insulation life. At this time, the corresponding fiber width is approximately 32 μm (79% of the width of the non-aging cardboard fiber), and the corresponding roughness is 0.225.

At the initial stage of aging, the fiber surface of the insulating board displays an "ablative" process, which may "ablate" the fibers on the surface of the insulating board [6], making the surface of the insulating board display a temporary smooth phenomenon (Figure 8b, degree of polymerization 993). With the extension of aging time, the fiber cell wall of the insulating paperboard begins to "peel" and display "crack silk separation"—cell wall displacement and deformation, where the outer layer of the primary wall and the secondary wall is broken and removed (Figure 8c, polymerization degree is 573). The fiber width decreases relatively, and a few holes appear on the surface (Figure 8d, polymerization degree is 469). A small amount of crystalline "solid" is accumulated (Figure 8e, degree of polymerization is 388), and the smoothness becomes worse. With the further aging of the insulating paperboard, part of the fibers began to break, and the fibers continued to be refined to produce more holes with a larger area than before (Figure 8f, degree of

polymerization is 352), and the surface became rougher, but the roughness rose slowly at this time.

There are more film-like substances on the surface of the unaged paperboard, which are arranged neatly and closely (Figure 8a). The fiber width is approximately 40.5 μm, and the degree of polymerization is approximately 1050.

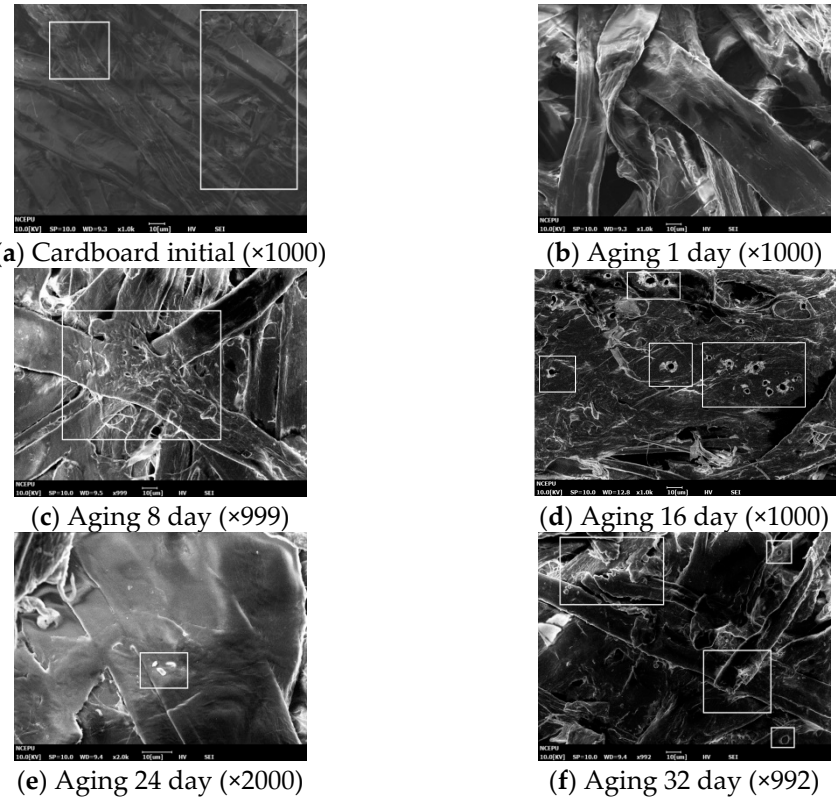

(**a**) Cardboard initial (×1000) (**b**) Aging 1 day (×1000)

(**c**) Aging 8 day (×999) (**d**) Aging 16 day (×1000)

(**e**) Aging 24 day (×2000) (**f**) Aging 32 day (×992)

Figure 8. SEM image of insulation cardboard with different aging times.

According to the description of the aging stages above, the overall microscopic morphology of the fiber width, surface roughness, and holes in the accelerated thermal aging process of insulating cardboard can be concluded, as shown in Table 2. It can be seen that with the increase in aging days, the filamentous material on the fiber surface decreases, the surface becomes smooth, and the number of holes gradually increases. Particles appear on the fiber surface and fiber morphology breaks.

Table 2. Variation of pressboard surface during different accelerated thermal aging durations.

Accelerated Thermal Aging Time/Day	Uptime/Year	Fiber Width/μm	Surface Roughness	Aging Characteristics of Cardboard
0	0	40.5	0.035	There are more filamentous substances on the surface of the fiber, which are arranged neatly and closely.
1	0.88	40.2	0.023	Filamentous material is reduced and the surface is relatively smooth.
8	7.06	38.2	0.086	The fibrous cell wall was displaced and deformed, and a few holes appeared.
16	14.12	36.5	0.192	The number of holes on the fiber increases, the area becomes larger, the life of cardboard is only half.
24	21.18	34.1	0.214	Particles appeared on the fiber surface.
32	28.24	33.2	0.222	The fiber fracture is serious and the holes are more obvious.
48	42.36	31.8	0.226	Most fiber fracture, serious surface damage, cardboard insulation life has reached the end.

5. Conclusions

(1) From an SEM image of cardboard after thermal aging image enhancement and denoising, segmentation, optimization, edge detection, corrosion, and expansion operation, the fiber width, hole size, and surface roughness data information can be extracted, through the quantitative analysis of SEM image information from the microscopic view, which is advantageous to the judgment of the aging condition of insulation board.

(2) The experimental study found that the surface morphology of insulating paper changed with the increase in thermal aging time, the number and area of the holes in the SEM of insulating paper also increased, and the internal fiber on the insulating paper also displayed the fracture phenomenon.

(3) The test shows that the aging state of cardboard can be roughly evaluated by the relationship between fiber width and surface roughness and the degree of polymerization, and the life of insulating cardboard can be roughly inferred. When the degree of polymerization is close to 500, that is, approximately 50% of the degree of polymerization of the original paperboard, the roughness is approximately 0.162, and the fiber width is 91% of the unaged board. The aging time can be roughly inferred to be approximately 14 days, and the insulation life is only approximately half. When the degree of polymerization is close to 250, that is, approximately 25% of the degree of polymerization of the original paperboard, the roughness is approximately 0.225, and the fiber width is 79% of the non-aging. The aging time can be roughly inferred to be approximately 45 days, close to the end of the insulation life. The aging state of insulating paper can be reflected by using the fiber width, roughness, and polymerization degree, which provides a new idea for testing the insulating properties of paperboard.

The digital twin model can be constructed to monitor the transformer bushwork in real-time, upload the running state of the insulating board through the cloud, process the obtained image of the insulating board, and calculate the roughness and fiber width of the insulating board, so as to estimate the aging degree and insulation life of the insulating board.

Author Contributions: Conceptualization, L.Z. and W.J.; methodology, Z.W.; software, Y.W. (Yongqiang Wang); validation, Y.W. (Yulong Wang), L.Z. and W.J.; formal analysis, Z.W.; investigation, L.Z.; resources, Y.W. (Yongqiang Wang); data curation, Z.W.; writing—original draft preparation, L.Z.; writing—review and editing, Y.W. (Yulong Wang); visualization, Y.W. (Yongqiang Wang); supervision, L.Z.; project administration, Z.W.; funding acquisition, W.J. All authors have read and agreed to the published version of the manuscript.

Funding: This research was funded by the Self-funded project of China Southern Power Grid Digital Grid Research Institute: Research on status assessment technology of substation equipment based on panoramic data fusion, grant number 670000KK52200137.

Conflicts of Interest: The authors declare no conflict of interest.

References

1. Liao, R.; Tang, C.; Yang, L. Research on the microstructure and morphology of power transformer insulation paper after thermal aging. *Proc. CSEE* **2007**, *27*, 59–64.
2. Luo, Z.; Dong, Y.; Hu, C. Statistic analysis on China electric reliability in 2008. *Electr. Power* **2009**, *42*, 8–12.
3. Verma, P.; Roy, M.; Verma, A.; Bhanot, V.; Pandey, O.P. Assessment of degradation of transformer insulation paper by SEM and X-RD techniques. In Proceedings of the 2004 IEEE International Conference on Solid Dielectrics, Toulouse, France, 5 July 2004.
4. Verma, P.; Roy, M.; Verma, A.; Bhanot, V. Assessment of degradation of transformer insulation paper by structural analysis. *J. Polym. Mater.* **2004**, *21*, 361–369.
5. Song, J.; Yue, B.; Xie, H. Study on multi-stress aging test system for stator winding insulation of large generator. *Proc. CSEE* **2000**, *20*, 9–13.
6. Liao, R.; Yan, J.; Yang, L.; Zhu, M.; Sun, C. Characteristics of partial discharge-caused surface damage for oil-impreganted insulation paper. *Proc. CSEE* **2011**, *31*, 129–137.
7. Yan, J.; Liao, R.; Yang, L.; Hao, J.; Sun, C. Analysis of damage products of oil-impregnated insulation paper caused by partial discharge. *Trans. China Electrotech. Soc.* **2011**, *26*, 184–191.

8. Miao, D. Study on Processing Method of SEM Soil Image Based on Matlab. Diploma Thesis, Taiyuan University of Technology, Taiyuan, Taiwan, 2014.
9. Wang, G.L.; Wu, C.W.; Dong, J.X.; Xie, X.S. The application of software photoshop in quantitative study on SEM photos. *J. Chin. Electron Microsc. Soc.* **2001**, *20*, 279–282.
10. Lian, H.; Ran, W.; Xia, X. Research on SEM image processing and micro-information extraction technology. *Coal Technol.* **2001**, *20*, 279–282.
11. Wang, B.; Shi, B.; Cai, Y.; Tang, C.-S. 3D visualization and porosity computation of clay soil SEM image by GIS. *Rock Soil Mech.* **2008**, *29*, 251–255.
12. Mao, L.; Xue, R.; An, L. Quantitative analysis on SEM image of microstructure with matlab. *J. Chin. Electron Microsc. Soc.* **2004**, *23*, 579–583.
13. Qi, B.; Tang, L.; Zhang, J. Research on measurement of hydrophobicity of insulators. *Proc. CSEE* **2008**, *28*, 121–124.
14. Yan, K.; Wang, F.; Zhang, Z.; Li, N.; Lv, F. Segmentation algorithm of hydrophobic image based on improved Canny operator. *High Volt. Appar.* **2014**, *50*, 97–101.
15. *GB/T1094.7-2008*; Loading Guide for Oil-Immersed Power Transformers. China Standard Press: Beijing, China, 1986.
16. Xie, J. Deterioration Rule and Diagnostic Method for Partial Discharge in Transformer Oil-Pressboard Insulation. Diploma Thesis, North China Electric Power University, Beijing, China, 2016.
17. Qin, L.; Chen, F.; Wang, G. Effects of fiber properties on the strength properties of paper. *Heilongjiang Pulp Pap.* **2004**, *32*, 11–12.
18. Pan, Q.; Yang, F.; Ye, L.; Liang, Y.; Cheng, Y.M. Survey of a kind of nonlinear filters-UKF. *Control. Decis.* **2005**, *20*, 481–489.
19. Daubechies, I. *Ten Lectures on Wavelets*; Society for Industrial and Applied Mathematics: Philadelphia, PA, USA, 1994; pp. 194–202.
20. Zhang, H.; Hou, D. An image segmentation algorithm based on iterative multiple threshold. *J. Shandong Norm. Univ.* **2016**, *33*, 49–56.
21. Yang, P.Z.; Jiang, S.W. The study on the 3D assessment of surface roughness. *Mach. Des. Res.* **2002**, *18*, 64–67.